Growth folding and shallow faults in the southern Puget Lowland, Washington State

Curtis R. Clement[1], Thomas L. Pratt[2], Mark L. Holmes[1], and Brian L. Sherrod[3]

[1]School of Oceanography, University of Washington, Seattle, WA 98195

[2]U. S. Geological Survey, School of Oceanography, University of Washington, Seattle, WA 98195

[3]U. S. Geological Survey, Department of Earth and Space Sciences, University of Washington, Seattle, WA 98195

Abstract

Marine seismic reflection data in southern Puget Sound, Washington State, show growth folding and probable Holocene scarps in the Tacoma Fault zone (Case and Carr Inlets), and image shallow faults near potential field anomalies associated with the Olympia Structure (Budd, Eld, and Totten Inlets). Beneath Case Inlet, the Tacoma fault zone includes a ~350-m-wide section of south-dipping strata forming the upper part of a fold (kink band) at the south edge of an uplifted shoreline terrace. A ~2 m change in the depth of the water bottom, onlapping post-glacial sediments, and increasing dips with increasing depth are consistent with growth folding and a late Pleistocene to Holocene fold scarp above a blind fault. Paleoseismic data across a similar, nearby fold scarp on land indicate recent uplift of probable Holocene age. Profiles acquired in Carr Inlet 10 km to the east showed Late Pleistocene or Holocene faulting at one location with ~3 to 4 m of vertical displacement, south side up. North of this fault, the data show several other disruptions and reflector terminations that could mark faults within the broad Tacoma fault zone. Seismic reflection profiles across part of the Olympia Structure in southern Puget Sound show two apparent faults about 160 m apart with 1 to 2 m of displacement of subhorizontal bedding. Directly beneath one of these faults, a dipping reflector that may mark the base of a glacial channel shows the opposite sense of throw, suggesting at least some strike-slip motion. These apparent faults indicate that the Tacoma fault and Olympia Structure include active faults and folds with possible Holocene motion.

Introduction

Active, shallow faults pose a seismic hazard to the 3.3 million people living in the Puget Lowland of northwest Washington State. Northeast directed subduction of the Juan de Fuca plate and northward motion of the Oregon Coast Range block deform the basement rocks beneath the Puget Lowland into a series of fault-bounded uplifts and basins (Pratt et al., 1997; Wells et al., 1998; Brocher et al., 2001; Johnson et al., 2004). The contrast between the sediment-filled basins and the areas of uplifted Crescent Formation volcanic rocks cause prominent gravity and magnetic anomalies that delineate west or northwest-trending faults, including the Southern Whidbey Island Fault (SWIF), Kingston Arch, Seattle Fault, Tacoma Fault, and Olympia Structure (Fig. 1; Gower et al., 1985; Finn, 1990; Finn et al., 1991; Johnson et al., 1994; Pratt et al., 1997; Brocher et al., 2001; tenBrink et al., 2002; Blakely et al., 2002; Johnson et al., 2004). These faults beneath the Puget Lowland are hypothesized to be part of an interconnected system (Pratt et al., 1997; ten Brink et al., 2002; Brocher et al., 2004; Johnson et al., 2004).

Although a M7+ earthquake has been documented on the Seattle fault in the central Puget Lowland about 1100 years ago (Bucknam et al., 1992; Nelson et al., 2003), the faults believed to bound the north and south edges of the Tacoma basin beneath the southern Puget Lowland have received less attention. On the north edge of the Tacoma basin, geophysical data show a west-trending series of faults and folds interpreted to be a broad Tacoma Fault zone (Pratt et al., 1997; Brocher et al., 2001; Booth et al., 2003; Johnson et al., 2004). Pratt et al. (1997) interpreted the central part of the Tacoma Fault zone as a south-dipping monoclinal fold or ramp later termed the "Rosedale Monocline" by Johnson et al. (2004), but tomographic models to the west suggest the Tacoma structure is a north-dipping reverse fault (Brocher et al., 2001). Johnson et al. (2004) interpreted the Tacoma Fault zone as an east-trending fault that crosses the Lowland, intersecting the northwest-trending Rosedale monocline beneath the central and east Lowland (Fig. 2a). Seismic reflection profiles across the west part of the Tacoma Fault zone beneath Case Inlet show a 360 m-wide kink band that appears to be a growth fold above a deeper fault (Fig. 2; Johnson et al., 2004).

The Olympia Structure at the south edge of the Tacoma basin (Fig. 1) remains enigmatic because the shallow inlets of southern Puget Sound prevent the collection of deep-penetration marine seismic reflection profiles across it (Pratt et al., 1997). The Olympia Structure separates

the 3.5 to 6.0 km of sedimentary strata in the Tacoma basin from uplifted Crescent Formation basement rocks exposed in the Black Hills south of the Lowland (Pratt et al, 1997; Brocher et al., 2001). Coincident gravity and magnetic gradients show the structure to be approximately 80 km long with a trend of about 315° (Fig. 1; Finn, 1990; Finn et al., 1991; Blakely et al., 1999). The linearity of the potential field anomalies suggests that the Olympia Structure is a fold or fault. Industry seismic reflection data at the northeast edge of the Olympia Structure show a gently north-dipping reflector, interpreted as the top of Crescent Formation basement rocks, overlain by nearly flat sedimentary strata of the Tacoma basin (Pratt et al. 1997). The south portion of the Olympia Structure, with the most prominent potential field anomalies, has not yet been imaged on seismic profiles. Pratt et al. (1997) proposed that the Olympia Structure is a ramp above the base of a fault, but this interpretation is not compelling because reflector onlap suggests that the Tertiary strata in the southern Tacoma Basin were deposited on a sloping surface with only slight folding (2° to 4° tilt) after deposition. Alternatively, the Olympia Structure could be a predominantly pre-Tertiary fold that is cut by a fault south of the existing industry seismic profiles.

Evidence for Holocene land-level changes at five locations along the Tacoma Fault and Olympia Structure suggest that there was a large earthquake about 1100 years ago in the southern Puget Lowland (Bucknam et al., 1992; Sherrod, 2001). Sherrod et al. (2004) document an uplifted tidal flat (terrace) at Case Inlet and a series of east-trending, south-facing, *en echelon* fault or fold scarps deforming the late Pleistocene to Holocene glacial deposits along the west part of the Tacoma Fault Zone (Fig. 2b). A trench dug across one of these scarps, the Catfish Lake scarp, showed a fold with more than 2 m of vertical relief, up to the north, but only minor faulting (< 30 cm; Sherrod et al., 2003, 2004). Their interpretation of the trench exposure is that the scarp is caused by warping of the post-glacial surface above a blind fault tip. Late Quaternary motion has not been convincingly documented on structures forming the central and eastern portions of the Tacoma fault zone, although Johnson et al. (2004) compiled evidence consistent with recent motion.

We collected shallow, high-resolution marine seismic reflection profiles across the west and central parts of the Tacoma fault zone and across the Olympia Structure to delineate faults or folds in the shallow strata and relate the paleoseismic observations to deeper structures. Pre-Quaternary strata beneath the Puget Lowland are largely covered by glacial deposits, the most

recent being from the Vashon stade of the Frasier glaciation that culminated about 16,400 years ago (Thorson, 1980; Booth, 1994; Porter and Swanson, 1998; Booth et al., 2004). These glacial deposits potentially record late Pleistocene and Holocene faulting, landsliding and ice-meltout. We also reexamined the data from the trench across the Tacoma Fault scarp just west of Case Inlet to relate the folding to that seen on the nearby seismic profiles. The profiles image a remarkable growth fold within the upper 30 m of the Tacoma Fault zone, above which there is vertical displacement of the water bottom. Paleoseismic studies suggest this displacement formed during an earthquake between A.D. 770 and 1160. Possible post-glacial faults were also observed cutting shallow strata along parts of the central Tacoma Fault zone and the Olympia Structure. The results thus document recent folding or faulting on both the north and south edges of the Tacoma basin.

Data Acquisition

We collected the single-channel, marine seismic reflection profiles using a sparker seismic source towed behind the University of Washington's *R/V WeeLander*. The waterways are nearly perpendicular to the major geophysical anomalies under investigation, so the main profiles were acquired along the shores or down the centers of the inlets.

During acquisition, we fired a 300-joule mini-sparker source every 0.5 s with a boat speed of about 6 km/hour. Single-channel seismic reflection data were collected using a 10-m-long hydrophone streamer. Digital data were recorded at 4000 samples/sec using a PC-based acquisition system (U.S. Geological Survey's Mudseis system). Record length was set at 0.25 sec, resulting in approximately 200 m maximum depth of penetration, but no reflectors were imaged at depths below about 150 m. Because of the high organic content of the bottom sediments in these shallow waterways, significant sub-bottom penetration along large stretches of some profiles was prevented by gas accumulations.

The data were bandpass filtered (300-1200 Hz), deconvolved, and migrated. Migrations utilized a Stolt f-k algorithm assuming a constant velocity of 1500 m/sec, as single-channel data do not provide accurate velocity information. The vessel's position was recorded at 5-sec intervals using differential GPS, giving an estimated location precision of about 6 m. This same seismic system, with a uniboom source comparable to the sparker source used here, has been

effective at imaging shallow strata in other seismically active regions (e.g., Pratt et al., 2001 and 2003b).

Growth folding within the western Tacoma fault zone

Our data across the western Tacoma fault in Case Inlet imaged gentle folding, a warped water bottom, and strata indicative of growth folding above a blind thrust or reverse fault. Johnson et al. (2004) document south-dipping strata in a 360-m-wide kink band beneath Case Inlet on deeper seismic reflection data (Fig. 2c). Our profiles image the kink band as a panel of south-dipping strata, with dips increasing downward to create a fanning sequence (Fig. 3a,b). The panel has a width of about 350 m on our profiles, but the south end is obscured by the onset of a strong reflector that is probably a gas-saturated layer near the water bottom. The north edge of the kink band is marked by a change from dipping to horizontal strata, as on the deeper seismic profile. Dips within the kink band increase downward to about 5º at a depth of about 40 m ("dipping reflector" in Fig. 3a,b). Johnson et al. (2004) show that the dips continue to increase to about 35º dip below at 300 m depth and below (~0.4 sec traveltime; Fig. 2c). The deeper profile is consistent with a fault extending to about 200 m depth (0.25 sec; Johnson et al., 2004). We propose that the shallow strata we imaged were deformed by growth folding and minor faulting above this active fault tip.

The water bottom is warped upward about 2 m above the center of the kink band (Fig. 3a,b), demonstrating Holocene fold growth. The warping forms a distinct, ~100-m-wide scarp on the water bottom. We interpret this scarp as forming the south edge of the uplifted terrace and tidal flat that lies north of the kink band, and to be the underwater extension of the en-echelon scarps visible on lidar data to the west (Fig. 2b).

Growth folding within the kink band beneath Case Inlet is consistent with geomorphic and paleoseismic observations made on the Catfish Lake scarp immediately to the west. A 30-m long trench across the scarp (Fig. 2b) exposed late Quaternary glacial sediments (till, sand, and gravel-filled channels), deposited by last-glacial ice sheets (Booth, 1994), and an oxidized surface soil developed on till (Fig. 3c). The oldest unit exposed in the excavation is a dense, sandy silt with abundant faceted gravel and cobbles. Clasts in the dense silt were imbricated in

many places, and displayed a crude stratification. The density, heterogeneity, and abundance of faceted clasts suggest that this deposit is lodgement till. A soil is developed in the uppermost part of the till and caps the exposed section. The deepest excavated soil horizon, a gray silty B/E horizon with platey structure, sits directly on the till surface. Immediately overlying the B/E horizon is a weakly developed B horizon (B_W) consisting of pale brown loamy sand to sandy loam. The uppermost horizon (A horizon) consists of dark brown lenses of organic material.

Deposits in the excavation showed evidence of postglacial folding and minor faulting. Deformation observed in the till is consistent with both glacial ice flow and movement on the Tacoma fault. Folding of till fabrics is defined by stratified pebbles and imbricated clasts. Pebble layers in the north half of the trench are almost horizontal whereas similar layers in the south half of the trench dip to the south. Imbricated clasts are more steeply inclined on the north side of fault F3 (Fig. 3c) and are almost subhorizontal to the south of F3. The break between the two fabric orientations occurs near F3, the fault that offsets a Holocene soil horizon, and both fabrics suggest anticlinal folding. However, the platy B/E horizon of the surface soil is displaced by a fault (F3) with ~30 cm of reverse offset. No organic material suitable for radiocarbon dating was present. Folded and faulted glacial deposits show that most of the deformation and scarp height postdate deposition by the ice sheet, which ended in this area about 16,400 years ago (Porter and Swanson, 1998).

The scarps beneath and west of Case Inlet coincide with shorelines that were uplifted in an earthquake between A.D. 770 and 1160. A raised tidal flat observed along the shores of Case Inlet north of the kink band indicates 4 m of late Holocene uplift (Fig. 2b). Raised tidal flat deposits north of the fault contain marine fossils. Paleoecology of the tidal-flat deposits and overlying upland soils require at least 1.5 m of uplift to change a tidal flat into a freshwater swamp or meadow (Bucknam et al., 1992; Sherrod, 2001). Ages of plant fossils within the tidal-flat deposits and from overlying freshwater peat limit uplift to between A.D. 770 and 1160 (Sherrod et al., 2004).

Radiocarbon ages from other uplifted or submerged coastal sites straddling the Tacoma fault also constrain the timing of deformation to between A.D. 770 and 1160. An age from leaf bases of *Triglochin maritima* that grew on a freshly uplifted tidal-flat surface at Lynch Cove (Fig. 2a) constrain uplift to shortly before A.D. 880–980. Similarly, freshwater peat deposited between A.D. 1000 and 770 at Burley (Fig. 2a) overlies sand vented onto a raised tidal flat,

implying that the ground shook hard enough to liquefy during uplift. At other sites, ages on freshwater swamp peat deposited over tidal-flat deposits loosely constrain uplift between A.D. 890 and 1410. A single age from a submerged tree south of the Tacoma fault constrains subsidence to between A.D. 980 and 1190. Sherrod (2001) and Sherrod et al. (2000 and 2004) also document coseismic submergence south of the Tacoma fault at Wollochet Bay (Fig. 2a) between 1010 and 1150 years ago.

The pattern of folding within the shallow strata beneath Case Inlet suggests that the kink band is a growth fold that initiated in the Quaternary. Horizontal strata in the upper 5 m onlap slightly south-dipping, post-glacial sediment layers in the upper 10 m of the kink band (Fig. 3a). The post-glacial strata beneath the onlap exhibit about 5 m of vertical change. A deeper, probably Late Pleistocene reflector has a dip of about 5º on our profiles and shows vertical relief of about 20 m across the kink band ("dipping reflector" in Fig. 3a,b). Upper Quaternary strata show the shallow fanning sequence, but deeper strata within the kink band appear to be parallel and therefore predate the folding (Fig. 2c; Johnson et al., 2004). The warping of the water bottom seen on the seismic reflection profile is similar in amplitude and wavelength to that at the Catfish Lake scarp to the west (Sherrod et al., 2003, 2004), and it lies at the south edge of the uplifted terrace. The data therefore are consistent with latest Pleistocene or Holocene growth of the kink band in response to motion on an underlying fault (Fig. 3d).

Other features on the Case Inlet seismic profiles have northeast trends that are approximately parallel to the glacial lineations (Fig. 4a) and are likely glacial in origin, although we cannot eliminate tectonic origins. One such feature beneath is a ~300 m wide ridge that appears to be onlapped by post-glacial sediments (Fig. 4b). On one profile this ridge is completely covered by undisturbed sediments, but on others its top is exposed and it has slight depressions on its edges (Fig. 4b). One interpretation is that this ridge formed by faulting, perhaps being the forelimb of a fault-propagation fold or a pop-up (flower) structure between two faults, with deformation releasing the gas from the overlying muds. However, a glacial origin is suggested by the strike of the feature being approximately parallel to the glacial lineations, at a high angle to the known fault scarps and geophysical anomalies (Fig. 4a). One possibility is that it is a glacially carved ridge like those on the surrounding land areas, and that tidal currents scour slight depressions on its margins and keep the overlying muds clear of gas.

A second feature obvious on the profiles is a change in water depth at the entrance to the northernmost arm of Case Inlet (Fig. 4c). This bathymetric step has a northeast trend that is approximately parallel to glacial features on the surrounding land. Again the step could be tectonic in origin, but the strike is at a high angle to the Tacoma fault and the geophysical anomalies, and does not coincide with the southern limit of the uplifted terrace. A simpler explanation is that the inlet is shallower towards its head, and this decrease occurs in steps that are controlled in part by the glacial ridges.

Shallow faults beneath Carr Inlet in the central Tacoma Fault Zone

Our Carr Inlet seismic profiles across the central Tacoma fault zone image strata that we interpret as Pleistocene glacial deposits covered by up to 20 m of late Pleistocene and Holocene sediments. The contact between these two units is a strong reflector that we interpret as an erosional unconformity, with the inferred Pleistocene glacial deposits beneath the unconformity having a hummocky appearance with discontinuous reflectors (Fig. 5a). Profiles perpendicular to the shorelines show the upper surface of these glacial deposits sloping gently toward the middle of the inlet, with the overlying subhorizontally stratified sediments onlapping this sloping surface. The late Pleistocene and Holocene sediments show slight folding or draping over the Pleistocene erosional surface. In many areas, including most of the deeper parts of the inlets, there was little signal penetration through a strong reflector within the shallow sediments (left side of Fig. 5a). We interpret this strong reflector as a gas-saturated layer.

Our Carr Inlet profiles show shallow, late Pleistocene or Holocene faulting near the Rosedale monocline. A clearly imaged fault, defined by abrupt changes in depth, possible diffractions, and folding of post-glacial sediments (Fig. 5a), lies within the flat-lying Tacoma basin strata about 3 km southwest of the axial surface at the base of the monocline (Fig. 2a; Pratt et al., 1997; Johnson et al., 2004). The shallow fault shows 3 to 4 m of vertical displacement on strata within the post-glacial deposits, south side up, and prominent diffractions that indicate truncations of strata (Fig. 5a). These diffractions were not entirely removed by migration, possibly because our estimated velocities are incorrect or the fault is oblique to the profile. The post-glacial strata on the south side of the fault are arched upward, but the water bottom does not appear to be deformed. Reflectors within the underlying glacial deposits show only slight disruptions at the fault, although the reflectors are hummocky and discontinuous by nature.

About 100 m to the south of the interpreted fault, diffractions and terminations of strong reflectors in the post-glacial sediments could mark another fault coincident with the abrupt onset of a gas-saturated layer (Fig. 5a).

We can not positively identify the fault on adjacent profiles, but two other potential faults lie to the northwest. One nearby feature is a disrupted area on the adjacent profile in which arching of the shallow layers is visible below a break in the strongly reflective, gas-saturated layer (Fig. 5b). One interpretation is that faulting caused the arching and released gas from the shallow layers; however, the disrupted area cannot clearly be attributed to a fault, nor can we eliminate the possibility that the two profiles are imaging separate structures. Another set of Late Pleistocene or Holocene faults may be imaged just north of the disrupted area (Figs. 2a and 5c). The possible faults are defined by steps, abrupt changes in dip, and changes of character in the strong unconformity reflector, which is flat and relatively featureless throughout most of the rest of the inlet. Reflectors are arched and abruptly change dip at the potential faults. There is also scattered energy that may be in part diffractions that are improperly migrated because we are crossing a fault obliquely. The water bottom does not appear to be disturbed above these faults, but we do not know the sedimentation rate (or erosion rate) to constrain the age.

If either of the latter features are the westward extension of the fault, it has a trend of about N40ºW, or nearly parallel to the axial surface inferred from deeper seismic data and potential field data (Fig. 2a). A fault is not interpreted on deeper seismic reflection profiles (Pratt et al., 1997; Johnson et al., 2004), perhaps because the total vertical displacement is less than the minimum resolution of the industry data. The fault also has not been identified in lidar data on the adjacent land (Fig. 2a). Thus, we interpret at least one fault beneath Carr inlet, but we cannot confidently relate it to nearby structures.

The axial surface at the base of the Rosedale monocline coincides with a change in slope and a possible disruption of the Late Pleistocene erosional surface, and with slight folding of the post-glacial sediments (Fig. 5d). The erosional unconformity is flat to the south of the axial surface, but is gently south-dipping to the north (2º dip; Fig. 5d). Coincident with the change in dip are 3 apparent faults that deform the post-glacial sediments and break the erosional surface into small blocks (~60 m wide) that have been uplifted or downdropped 1 to 2 m. The change in dip of the erosional surface is suggestive of folding at the axial surface, but it could equally well be unrelated to tectonic activity. Specifically, the change in dip could be related to the sloping

side of the channel, with our survey fortuitously crossing the slope break near the axial surface. The post-glacial sediments onlap horizontally onto the dipping surface (Fig. 5d), suggesting that the tilting predates the post-glacial sediments. The disruptions in the Late Pleistocene surface and the slight folding of the post-glacial sediments suggest Late Pleistocene or Holocene faulting.

The inferred faults beneath Carr Inlet in the central Tacoma fault zone could be the shallow expression of deep faults, or could be small, unrooted faults related to growth folding of the underlying monocline. The base of the Rosedale monocline appears as a synclinal axial surface on industry seismic data, without clear evidence of faults penetrating the dipping strata in the limb of the fold (Pratt et al., 1997). This implies that the shallow faults we imaged either have a total vertical displacement that is smaller than the limit of resolution on the industry data, or that the faults are minor bending-moment faults. However, the latter still would provide evidence for late Pleistocene or Holocene growth of the fold, which requires motion on underlying faults.

The apparent faults we imaged beneath Carr Inlet are unlikely to be caused by landslides. Some lie near the center of the broad inlet with little relief on the water bottom, and far enough from the shoreline to be beyond the toe of even deep-seated landslides. More problematic is the possibility that the shallow faults are due to compaction or settling, as the area was covered by ice during the last glaciation. A tectonic origin is consistent with their location above a large fold (the Rosedale monocline) that may be associated with deep, active faults in the region (Pratt et al., 1997; Johnson et al., 2004).

Shallow faulting within the Olympia Structure

Our seismic surveys across the Olympia Structure provide images of apparent faults cutting sub-glacial or post-glacial strata of late Pleistocene or Holocene age (Fig. 6). Our profiles from Budd Inlet show small basins or channels up to 3.5 km across and 140 m deep that are characterized by dipping reflectors at their base, which we interpret as erosional unconformities, overlain by subhorizontally layered strata. Geologic maps show the surrounding points of land to be pre-Vashon deposits (>16,400 years old) along the shorelines, overlain by Vashon till (e.g., Palmer et al., 1999). Extensive, deep channels were cut into these pre-Vashon deposits beneath the glaciers (e.g., Booth, 1994; Booth et al., 2004), and many of these channels were filled with

subglacial and unconsolidated recessional deposits as the glacier retreated about 16,400 years ago (Porter and Swanson, 1998).

Faults appear to cut the interpreted subglacial and recessional deposits imaged on our profiles across the Olympia Structure. Our profile from north-central Budd Inlet shows a channel feature defined by a north-dipping reflector (an erosional surface) beneath a horizontally layered sequence (Fig. 6c). Within the layered sequence, two faults appear to cut a 20-m-thick packet of prominent reflectors between 50 and 70 m depth. The first fault is expressed on our eastern profile as a 10-m-wide sag feature with sedimentary strata on the north side lying 1 to 2 m deeper than equivalent strata to the south. The depression may be caused by minor extension or by compaction from dewatering within a fault zone. The fault may extend to within a few m of the water bottom, where reflectors appear to be disrupted. The dipping reflector marking the unconformity at the base of the horizontal strata is displaced 1 to 2 m with the opposite sense of motion (up to the north) than the overlying strata. The differing senses of displacement on reflectors of different depths indicate either strike-slip motion, or reactivation of the fault with a different sense of displacement. We favor the strike-slip interpretation because we do not expect the stress regime to have changed significantly during the Quaternary.

On the northwest side of Budd Inlet, a nearly parallel seismic profile shows a similar sag feature (Fig. 6d) that could be the westward extension of the one just described. The sag feature on the western profile is clearly imaged extending into the shallowest strata just below the water bottom. The sagging is more pronounced, possibly indicating greater displacement or more extension on this part of a fault. A fault connecting the two sag features would have a strike of about 285°, which differs significantly from the 315° strike of the Olympia Structure (Fig. 6a). However, the potential field anomalies show a variety of strikes in the Black Hills (Fig. 1), and this may indicate the presence of faults of several orientations.

Our eastern Budd Inlet profile shows what could be another fault with about 2 m of vertical displacement approximately 160 m to the north of the sag feature (Fig. 6c). This apparent fault appears as a ~20 m wide non-reflective zone, with the prominent layered sequence lying about 2 m deeper on the north side. Reflector truncations and a notch in the water bottom suggest recent motion may cut the shallowest strata. A comparable fault is not obvious on the adjacent profile, but the fault could pass through the non-reflective area about 200 m north of the sag feature.

The sense of vertical displacement of the layered sequence on both of the faults beneath Budd Inlet, up to the south, is consistent with the long-term motion that downdropped the Tacoma basin and brought Eocene Crescent Formation rocks to the surface in the Black Hills. We may be imaging multiple strands of a thrust or reverse fault, or *en echelon* strike-slip faults.

We interpret the features described above as faults rather than deformation caused by compaction during glaciation or by rebound after the glaciers receded. The main arguments for a tectonic origin are the differing senses of displacement on reflectors of different depth (Fig. 6c) and the coincidence of the apparent faults with a major tectonic feature defined by the south edge of the Tacoma Basin and potential field anomalies. Glacial features would produce shallow faults in which all strata show the same sense of displacement. Also, if our interpretation of the stratigraphy is correct, the subhorizontal strata are recessional deposits that have not been compressed by glacial ice. A second possibility is a deep-seated slide feature, but the lack of steep topography perpendicular to the trend of the sag feature argues against a slump or landslide.

Topographic (lidar) data also may show evidence for the faults we imaged on the seismic data, consistent with motion since the last glaciation ~16,400 years ago (Thorson, 1980; Porter and Swanson, 1998). The trend of our interpreted fault through the sag feature extends to near a faint lineament visible in lidar topographic data approximately 2 km to the west (Fig. 6a,b). This lineament shows only a slight elevation change, and would not normally be identified as a fault scarp because of the lack of a vertical offset across it. Its main expression consists of stream valleys that appear to be aligned along it. However, the apparent faults in the seismic data have only 1 to 2 m of vertical displacement, and the predominant motion may be strike slip. A second, parallel lineament, also weakly expressed but including stream valleys, lies about 1 km farther south. These topographic lineations are far more subdued than the fault scarps evident in lidar data to the north (e.g., Sherrod et al., 2004; Fig. 2b), but their location along the projected trend of apparent faults makes them suspect.

The shallow faults found in our surveys could be the surface expression of a major fault in the basement rocks (the hypothesized Olympia fault), or they could be shallowly-rooted, bending-moment faults accommodating folding in the underlying basement rocks. The latter explanation would be consistent with the interpretation of Pratt et al. (1997), including a slight change in dip angle (~2° to 4°) at the south end of the Tacoma basin. However, given the

tectonic setting with several major thrust or reverse faults beneath the Puget Lowland, an equally likely possibility is that the Olympia Structure is a south-dipping thrust or reverse fault like the Seattle fault, and that the apparent faults we image are at the north edge of this major fault zone.

The faulted, subhorizontal beds that we imaged are likely post-glacial strata filling a channel, which implies late Pleistocene or Holocene faulting. The 10 to 30 m of burial for the reflector sequence requires a Holocene age if we assume the average deposition rate in southern Puget Sound of 0.5 – 3.5 cm/yr (Carpenter et al., 1985; Lavelle et al., 1986). However, all of the subhorizontal strata we imaged may have been deposited very soon after the late Pleistocene glaciation, when the deposition rate was likely much higher than now. The faults have possibly been active since the Miocene or Oligocene, as the 3.5 to 6 km of vertical change in the elevation of the Crescent Formation between the Black Hills and the Tacoma basin suggests long-term motion like that on the major fault zones to the north (e.g., Johnson et al., 1994; Pratt et al., 1997; ten Brink et al., 2002). The industry data do not extend far enough to the south to see whether deeper strata are broken by faults (Pratt et al., 1997).

Discussion

Tacoma Fault Zone. Our results from Case Inlet suggest that the scarps apparent on the lidar data in the western Tacoma fault zone are growth folds rather than surface ruptures. This hypothesis means that trenches across the scarps will exhume only minor faults accommodating the folding, as seems to be the case with the Catfish Lake scarp described here. Interpretation of past events rests in part on interpreting the fold growth through dating of growth strata. A combination of shallow seismic reflection data to define the fold geometry and coring to obtain samples for dating the growth strata on folds has been used successfully to obtain ages of past events on growth folds in the Puente Hills fault zone in Los Angeles (Pratt et al., 2002; Dolan et al., 2003). These same methods of growth analysis presumably could be applied in the Puget Lowland region.

We propose that the kink band we imaged in Case inlet formed in the Quaternary above a steeply-dipping reverse or oblique-slip fault (Fig. 3d). The vertical displacement across this kink band on the deeper Quaternary layers is relatively small (~300 m; Johnson et al., 2004). The amount of pre-Quaternary displacement on the fault is unknown, but potential field data (Fig. 1; Pratt et al., 1997), tomographic data (Brocher et al., 2001), and its location at the north edge of

the Tacoma basin suggest substantial displacement. We cannot determine amounts of strike-slip motion, if any, except that it is too small to be obvious in the late Pleistocene to Holocene surface features.

Recent uplift in the last event, as denoted by the change in depth of the water bottom, is concentrated in the central or north-central part of the kink band. Johnson et al. (2004) interpret the kink band as an upward-narrowing growth triangle. However, the seismic profiles seem to show a fanning of reflector dips like that expected in progressive limb rotation (Hardy and Poblet, 1994). The narrower uplift of the water bottom raises the possibility of an alternative growth mechanism in which the kink band is the sum of a number of narrower folds. The kink band would thus grow in discreet increments both vertically and horizontally.

Within the central Tacoma Fault zone, the faults we imaged demonstrate post-glacial motion at the south edge of the Seattle Uplift. Such motion was known in the west part of the Tacoma fault because of the lidar scarp and the land-level changes documented previously (Sherrod et al., 2004). In the case of the fault we imaged beneath central Carr inlet, the latest deformation has a sense of motion (south side up; Fig. 5a) opposite to the long-term trend, requiring a backthrust if the fault is part of a deep structure. The faults in the central Tacoma fault zone beneath Carr inlet may be part of the broader deformation zone, perhaps a backthrust or part of a shallow roof thrust as proposed by Brocher et al. (2004). One possibility is that a deep thrust or reverse fault ruptures in major earthquakes, with most of the deformation being consumed by folding and only a small part of the motion reaching the surface as faults. These small faults distribute the deformation over a broad zone, and are not visible on deeper seismic reflection profiles (Pratt et al., 1997) because their displacement is less than the resolution of the data. Another alternative is that the faults we imaged are small faults associated with bending at the synclinal axial surface. In this interpretation, the faults would have little displacement and would sole into bedding planes at shallow depths. Such faults could be very limited in their lateral extent and could have opposite senses of displacement. A final alternative is that the Rosedale monocline and the faults are responses to two different stresses – the fold forming in response to thrusting and the faults being caused by strike-slip motion parallel to the axial surfaces of the monocline.

The presence of the faults and folds in areas where the gas-saturated layers are missing in Carr and Case Inlets suggests a relationship between the faults and the gas deposits. Deformation

associated with the faults and folds may have released or prohibited the formation of gas accumulations, leaving windows of signal penetration along the faults. This implies that the distribution of windows through the gas layers could be used to identify areas of recent faulting above other active fault zones.

Olympia Structure. Our study documented the presence of active faults within the broader Olympia Structure beneath the south end of the Puget Lowland. Whether the faults we imaged are at the tip of a major fault zone or are small bending-moment faults within a fold, they require late Pleistocene to Holocene motion on faults either within or beneath the structure. Active faults are consistent with the large geophysical anomalies and the land-level changes along the Olympia Structure (Gower et al., 1985; Finn, 1990; Finn et al., 1991; Bucknam et al., 1992; Sherrod, 2001).

If the shallow faults beneath northern Budd Inlet are related to a major structure, they are likely splays that lie north of the fault that has the largest displacement of basement rocks. A pronounced gravity gradient spans the length of the inlet (Finn et al., 1991), and the abrupt change in magnetic anomalies from low-frequency in the northeast to high-frequency in the southwest occurs beneath the central or southern part of Budd Inlet, several km south of the shallow faults (Fig. 1). If these potential field anomalies are related to a major fault in the basement rocks, as seems likely, the faults we imaged beneath northern Budd Inlet lie several km north of this major basement structure.

The locations of our profiles in Budd Inlet are south of the industry seismic profiles in Puget Sound, the southernmost of which shows a strong, north-sloping reflector that has been interpreted as the top of Crescent Formation (Pratt et al., 1997). This reflector lies at slightly more than 1 km depth at the south end of the industry profile, about 2 km north of the faults we imaged. Based on the slope seen on the industry data, the basement reflector probably lies at about 800 m depth beneath the faults we imaged, and at about 200 m depth beneath the south end of the inlet. However, the sloping reflector projects to sea level at a location where basement rocks lie at an elevation of about 200 m in the Black Hills south of Budd Inlet, which suggests that a fault with at least 200 m of vertical throw could lie beneath southern Budd Inlet. A logical interpretation is that we are imaging a splay fault that lies several km northeast of a thrust fault that lifts Crescent Formation rocks to the surface in the Black Hills. We do not see obvious

deformation at the location of the main fault, but there is little or no signal penetration in our other profiles across the structure.

Conclusions

In the western Tacoma fault zone, our shallow seismic data show distinct growth strata above a narrow (360 m) kink band visible in deeper strata on previously published data. Onlapping of post-glacial strata onto older surfaces, apparent warping of the water bottom, correlation with scarps, and an uplifted marine terrace north of the kink band are consistent with a large earthquake about 1100 years ago. The growth folding within the kink band shows continued motion on the kink band in the Quaternary, although older strata at depths of about 300 m do not appear to show growth folding.

Within the central Tacoma fault zone, our seismic reflection profiles show shallow, post-glacial faults above the Rosedale monocline. We interpret one fault with south-side-up motion to cut post-glacial strata just south of the monocline, and other faults that appear to cut pre-Vashon glacial deposits and warp post-glacial strata appear to lie near the synclinal axis of the monocline. The relationship between these faults and the monocline visible on deeper data is unknown, but they may be small faults cutting through the monocline, or bending-moment faults formed in response to continued growth of the monocline.

Our high-resolution seismic reflection surveys document a late Pleistocene to Holocene fault within the Olympia Structure. Two sag features are visible on seismic profiles from both sides of Budd Inlet. These features align with weak lineaments visible nearby in lidar data, although these lineaments are not clearly identifiable as scarps. A second fault is imaged about 100 m north of the sag feature. Taken together, these data indicate that the Olympia Structure includes late Quaternary faults having a trend of about 285°. This trend differes from the 315° trend of the potential field anomalies related to the Olympia Structure. The lineaments and the likely post-glacial age of the strata visible on the seismic profiles suggest late Pleistocene or Holocene motion along the fault. Although the shallow strata are displaced down to the north, strike-slip motion also is suggested from the seismic profiles because of the opposite sense of displacement seen on reflectors at different depths. These faults could be the tip of deep-seated faults, or they could be bending-moment faults within a broad fold. In either case,

documentation of faults cutting the late Pleistocene to Holocene strata indicates the structure poses an earthquake hazard.

Acknowledgments.

John Crouch was instrumental in acquiring and helping analyze the Tacoma fault portions of the data. Funding for this project was provided by the School of Oceanography, University of Washington, as part of senior research projects by John Crouch and Curtis Clement. Dave Thoreson operated the *R/V Wee Lander* under challenging weather and sea conditions, and Floyd McCroskey kept equipment maintained and ready for use. Dick Sylwester of Northwest Geophysical Services provided some of the seismic system components. LiDAR data were provided courtesy of the Puget Sound LiDAR Consortium. Magnetic data were provided by R. Blakely of the U.S. Geological Survey. We thank Derek Booth and Ralph Haugerud for their suggestions for improving the manuscript.

References

Blakely, R.J., R.E. Wells and C.S. Weaver (1999). Puget Sound aeromagnetic maps and data, *U. S. Geological Survey Open-File Report 99-514*. (http://pubs.usgs.gov/of/1999/of99-514/)

Blakely, R.J., R.E. Wells, C.S. Weaver, and S.Y. Johnson (2002). Location, structure, and seismicity of the Seattle fault zone, Washington: Evidence from aeromagnetic anomalies, geologic mapping, and seismic-reflection data, *Geol. Soc. Am. Bulletin* **114**, 169-177

Booth, D. B. (1994). Glaciofluvial infilling and scour of the Puget Lowland, Washington, during ice-sheet glaciation. *Geology* **22**, 695-698.

Booth, D.B., K.G. Troost, J.J. Clague and R.B. Waitt (2004). The Cordilleran Ice Sheet: Chapter 2 in A. Gillespie, S.C. Porter and B. Atwater, eds., *The Quaternary Period in the United States*, International Union for Quaternary Research, Elsevier Press, p. 17-43.

Brocher, T.M., T. Parsons, R.J. Blakely, N.I. Christensen, M.A. Fisher, R. E. Wells, and the SHIPS working group (2001). Upper crustal structure in Puget Lowland, Washington: Results from the 1998 Seismic Hazards Investigation on Puget Sound, *J. Geophys. Res.* **106**, 13541 – 13564.

Brocher, T.M., R.J. Blakely, and R.E. Wells (2004). Interpretation of the Seattle Uplift, Washington, as a passive roof duplex, *Bull. Seismol. Soc. Amer.* **94**, 1379-1401.

Bucknam, R.C., E. Hemphill-Haley, and E.B. Leopold (1992). Abrupt uplift within the past 1700 years at southern Puget Sound, Washington, *Science* **258**, 1611 – 1614.

Carpenter, R., M. L. Peterson, and J. T. Bennett (1985). ^{210}Pb-derived sediment accumulation and mixing rates for the greater Puget Sound region, *Marine Geology* **64**, 291-312.

Dolan, J. F., S. A. Christofferson and J. H. Shaw (2003), Recognition of paleoearthquakes on the Puente Hills blind thrust fault, California, *Science* **300**, 115-118 [DOI: 10.1126/science.1080593]

Finn, C. (1990). Geophysical constraints on Washington convergent margin, *Journal of Geophysical Research* **95**, p. 19,553-19,546.

Finn, C., W.M. Phillips, and D.L. Williams (1991). Gravity anomaly and terrain maps of Washington, *U.S. Geol. Surv. Geophys. Invest. Map* **GP-988**.

Gower, H. D., J.C. Yount, and R. S. Crosson (1985). Seismotectonic map of the Puget Sound region, Washington, *U.S. geol. Surv. Misc. Invest. Ser. Map* **I-1613**.

Haeussler, P. J., and K. P. Clark (2000). Preliminary geologic map of the Wildcat Lake 7.50 quadrangle, Kitsap and Mason Counties, Washington, scale 1:24,000, *U.S. Geol. Surv Open File Rep*, **00-356**.

Hardy, S., and J. Poblet (1994). Geometric and numerical model of progressive limb rotation in detachment folds, *Geology* **22**, 371-374.

Haugerud, R.A., and Harding, D.J. (2001). Some algorithms for virtual deforestation (VDF) of LiDAR topographic survey data, *International Archives of Photogrammetry and Remote Sensing* **XXXIV-3/W4**, p. 211–217. http://duff.geology.washington.edu/data/raster/lidar/vdf4.pdf (March 2003).

Haugerud, R.A., D.J. Harding, S.Y. Johnson, J. Harless, C.S. Weaver, and B.L. Sherrod (2003). High-resolution LiDAR topography of the Puget Lowland, Washington – A bonanza for earth science, *GSA Today* **13** (6), 4-10.

Johnson, S.Y., C.J. Potter, and J.M. Armentrout (1994). Origin and evolution of the Seattle fault and Seattle basin, Washington, *Geology* **22**, 71-74.

Johnson, S.Y., R.J. Blakely, W.J. Stephenson, S.V. Dadisman, and M.A. Fisher (2004). Active shortening of the Cascadia forearc and implications for seismic hazards of the Puget Lowland, *Tectonics* **23**, TC1011, doi 10.1029/2003TC001507.

Lavelle, J. W., G. J. Massoth, and E. A. Crecelius (1986). Accumulation rates of recent sediments in Puget Sound, Washington, *Marine Geology* **72**, 59-70.

Nelson, A.R., S.Y. Johnson, H.M. Kelsey, R.E. Wells, B.L. Sherrod, S.K. Pezzopane, L.A. Bradley, R.D. Koehler and R.C. Bucknam (2003). Late Holocene earthquakes on the Toe Jam Hill fault, Seattle fault zone, Bainbridge Island, Washington, Geological Society of America Bulletin, 115 (11), 1388-1403.

Palmer, S.P., T.J. Walsh, and W.J. Gerstel (1999). Geologic Folio of the Olympia-Lacey-Tumwater Urban area, Washington: Liquefaction Susceptibility Map, *Washington State Department of Natural Resources Geologic Map* **GM-47**.

Porter S.C. and T.W. Swanson (1998). Radiocarbon age constraints on rates of advance and retreat of the Puget lobe of the Cordilleran ice sheet during the last glaciation, *Quaternary Research* **50**, 205-213.

Pratt, T.L., S. Johnson, C. Potter, W. Stephenson and C. Finn (1997). Seismic reflection images beneath Puget Sound, western Washington State: The Puget Lowland thrust sheet hypothesis, *J. Geophys. Res.* **102**, 27469-27489.

Pratt, T.L., Odum, J., Stephenson, W., Williams, R., Dadisman, S., Holmes, M., and Haug, B. (2001). Late Pleistocene and Holocene tectonics of the Portland Basin, Oregon and Washington, from high-resolution seismic profiling, *Bulletin of the Seismological Society of America* **91**, 637-650.

Pratt, T.L., J.H. Shaw, J.F. Dolan, S. Christofferson, R.A. Williams, J.K. Odum, and A. Plesch (2002). Shallow seismic imaging of folds above the Puente Hills blind-thrust fault, Los Angeles, California, *Geophysical Research Letters* **29**, 18-1 to18-4.

Pratt, T.L., Brocher, T.M., Weaver, C.S., Miller, K.C., Trehu, A.M., Creager, K.C., and Crosson, R.S. (2003a). Amplification of seismic waves by the Seattle basin, Washington State, *Bulletin of the Seismological Society of America* **93**, 533-545.

Pratt, T.L., Holmes, M., Schweig, E.S., Gomberg, J., and Cowan, H.A. (2003b). High resolution seismic imaging of faults beneath Limón Bay, northern Panama Canal, Republic of Panama, *Tectonophysics* **368**, 211-227.

Pratt, T.L., and Brocher, T.M. (2006). Site response and attenuation in the Puget Lowland, Washington State, *Bulletin of the Seismological Society of America* **96**, 536-552.

Sherrod, B. L., R.C. Bucknam and E.B. Leopold (2000). Holocene relative sea level changes along the Seattle Fault at Restoration Point, Washington, *Quat. Res.* **54**, 384-393.

Sherrod, B. L. (2001). Evidence for earthquake-induced subsidence about 1100 yr ago in coastal marshes of southern Puget Sound, Washington, *GSA Bulletin* **113**, 1299-1311.

Sherrod, B.L., A. Nelson, H. Kelsey, T. Brocher, R. Blakely, C. Weaver, N. Rountree, S. Rhea and B.S. Jackson (2003). The Catfish Lake scarp, Allyn, Washington: Preliminary field data and implications for earthquake hazards posed by the Tacoma fault, *U.S. Geological Survey Open-File Report* **03-455**.

Sherrod, B. L., T. M. Brocher, C.S. Weaver, R. C. Bucknam, R. J. Blakely, H. M. Kelsey, A. R. Nelson and R. Haugerud (2004). Holocene fault scarps near Tacoma, Washington, USA, *Geology* **32**, 9-12.

ten Brink, U.S., P.C. Molzer, M.A. Fisher, R.J. Blakely, R.C. Bucknam, T. Parsons, R.S. Crosson, and K.C. Creager (2002). Subsurface geometry and evolution of the Seattle Fault Zone and Seattle Basin, Washington, *Bull. Seism. Soc. Am.* **92**, 1737-1753.

Thorson, R. M. (1980). Ice-Sheet Glaciation of the Puget Lowland, Washington, during the Vashon Stade (late Pleistocene), *Quat. Res.* **13**, 303-321.

Van Wagoner, T. M., R. S. Crosson, K. C. Creager, G. Medema, L. Preston, N. P. Symons, and T.M. Brocher (2002). Crustal structure and relocated earthquakes in the Puget Lowland, Washington from high resolution seismic tomography, *J. Geophys. Res.* **107**, B12, ESE 22-1 to ESE 22-23 [joi:10.10129/2001JB000710].

Wells, D.L. and K.J. Coppersmith (1994). New empirical relationships among magnitude, rupture length, rupture width, rupture area, and surface displacement, *Bulletin of the Seismological Society of America* **84**, 974-1002.

Wells, R., C. Weaver, and R. Blakely (1998). Fore-arc migration in Cascadia and its neo-tectonic significance, *Geology* **26**, 759–762.

School of Oceanography, Box 357940
University of Washington
Seattle, WA 98195-7940
clement@u.washington.edu
(C.R.C, M.L.H.)

U. S. Geological Survey
School of Oceanography, Box 357940
University of Washington
Seattle, WA 98195-7940
(T.L.P.)

U. S. Geological Survey
Department of Earth and Space Sciences, Box 351310
University of Washington
Seattle, WA 98195-1310
(B.L.S.)

Figures.

Figure 1. Magnetic map from Blakely et al. (1999) showing the major faults and folds beneath the Puget Lowland (red labels and black arrows). The black rectangles show the Olympia and Tacoma study areas. Red dashed lines outline the Tacoma, Seattle and Everett basins, as determined by the 4.25 km/sec contour on a tomography image at 2.5 km depth (Van Wagoner et al., 2002).

Fig. 2. a,b) Lidar maps of the Tacoma Fault zone showing the scarps and trench west of Case Inlet, the location of the kink band (white dashed lines labeled 'A') imaged on seismic reflection data (Johnson et al., 2004), the terrace surrounding the north end of the inlets, and the tracklines for our seismic reflection profiles (thin black lines). Numbers and letters indicate figure numbers that show the indicated features. WB=Wollochet Bay. c) Seismic reflection profile from Johnson et al. (2004) showing kink band beneath Case Inlet. Black dots show interpreted base of Quaternary strata.

Figure 3. Growth folding at Case Inlet and at the trench west of the inlet. a,b) Parallel seismic reflection profiles (see figure 2 for location) showing growth folding, onlap of shallow strata, and warped water bottom at the top of the kink band. c. Trench log showing the folding and minor faulting discussed in the text. d. Kinematic model showing the kink band to be growth folding above a buried fault.

Figure 4. a) Lidar map of Case Inlet and surrounding region showing the locations of probable glacial features (white dashed lines) visible on the seismic profiles and shown in parts b and c. They are likely glacial in origin because their trends are nearly the same as the glacial lineations.

Figure 5. Shallow faults beneath Carr Inlet. See figure 2 for locations. a) Shallow fault that appears to cut post-glacial strata. b) Disruption that allows signal penetration through the shallow, gas-saturated layer. A fault is one potential explanation for the disruption. c) Apparent faults disrupting the unconformity at the base of post-glacial deposits(?). d) Apparent faults and change in dip of the unconformity at the axial surface of the Rosedale Monocline.

Figure 6. Shallow faults beneath Budd Inlet. Index map shows location relative to the Tacoma Fault (TF), the Seattle Fault (SF) and the Rosedale Monocline (shaded). a) Lidar map shows the locations of our seismic profiles in Budd, Totten and Eld Inlets (black lines). White dots are the locations of faults shown on lower seismic sections. White rectangle shows the location of map 'b' showing lineaments. Lower figures show east (c) and west (d) profiles from the north end of Budd Inlet, with sag feature and transparent zone that we interpret as faults (white dashed lines).

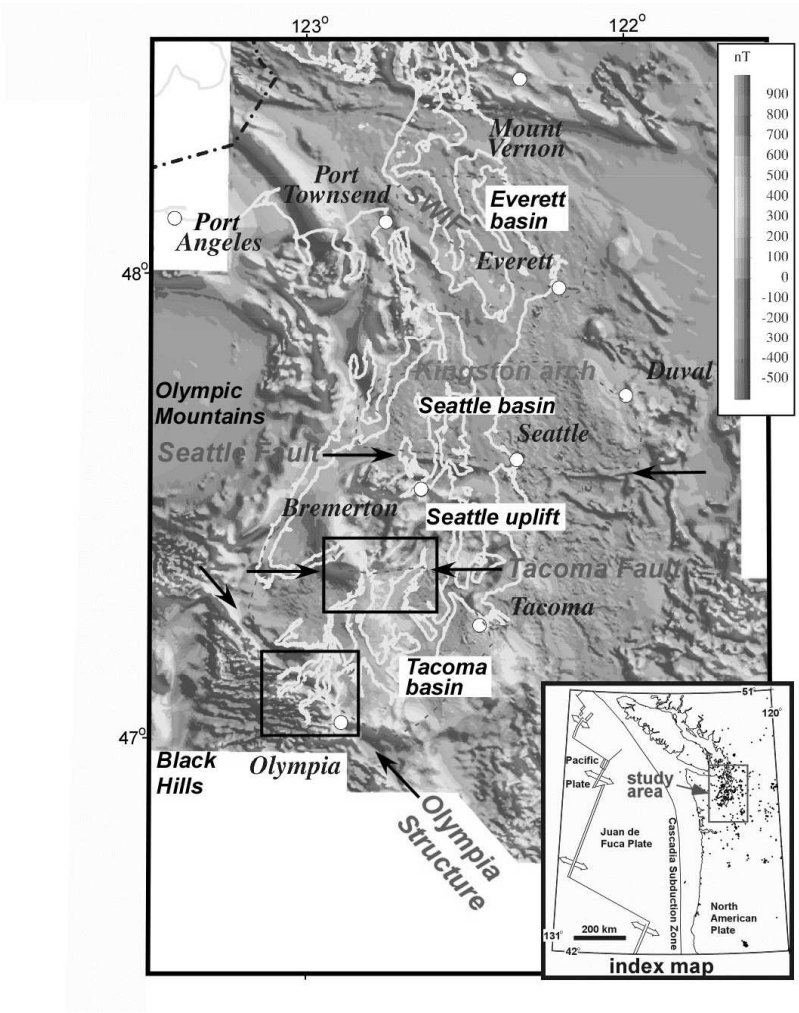
123°
122°
48°
47°
nT
900
800
700
600
500
400
300
200
100
0
-100
-200
300
-400
-500
Mount Vernon
Port Townsend
Port Angeles
Everett basin
Everett
Kingston arch
Duval
Olympic Mountains
Seattle basin
Seattle
Seattle Fault
Bremerton
Seattle uplift
Tacoma Fault
Tacoma
Tacoma basin
Black Hills
Olympia
Olympia Structure
index map
Pacific Plate
study area
Juan de Fuca Plate
Cascadia Subduction Zone
North American Plate
200 km
51°
120°
131°
42°

Figure 1.

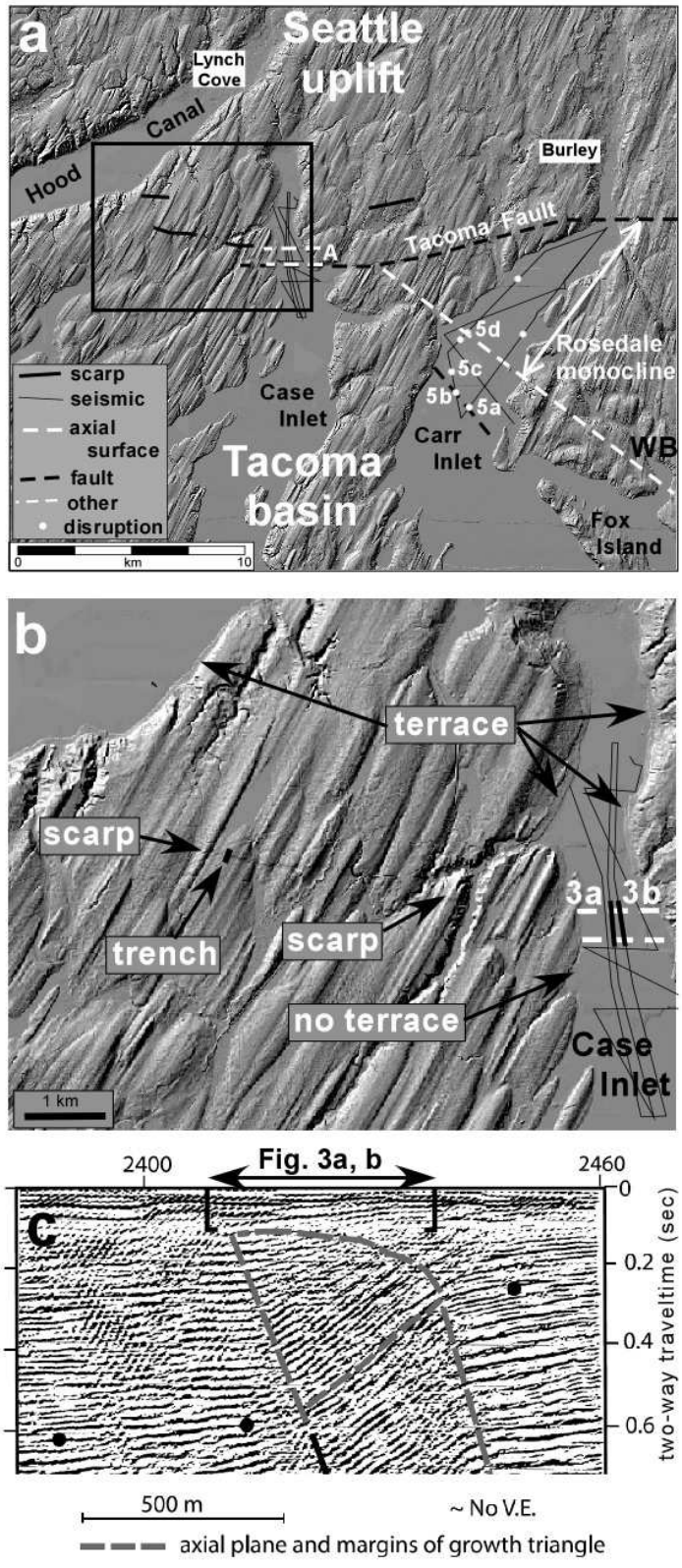
a
Seattle uplift
Lynch Cove
Canal
Hood
Burley
Tacoma Fault
A
5d
5c
5b
5a
Rosedale monocline
Case Inlet
Carr Inlet
Tacoma basin
WB
Fox Island
scarp
seismic
axial surface
fault
other
disruption
0
km
10
b
terrace
scarp
trench
scarp
3a
3b
no terrace
Case Inlet
1 km
c
2400
Fig. 3a, b
2460
0
0.2
0.4
0.6
two-way traveltime (sec)
500 m
~ No V.E.
axial plane and margins of growth triangle

Figure 2.

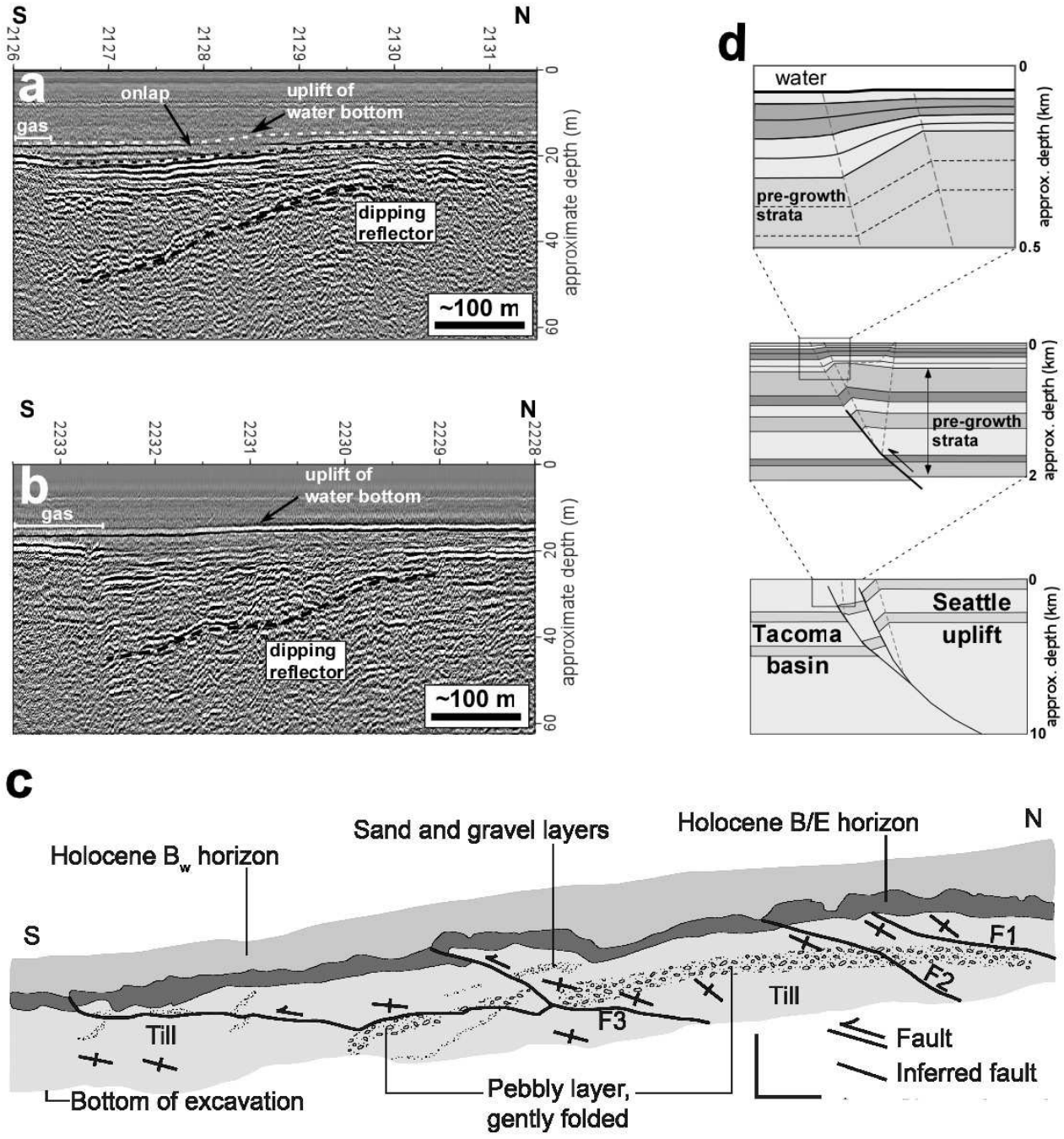
a
S
N
2126
2127
2128
2129
2130
2131
onlap
uplift of
water bottom
gas
dipping
reflector
~100 m
approximate depth (m)
b
2233
2232
2231
2230
2229
2228
uplift of
water bottom
gas
dipping
reflector
~100 m
d
water
pre-growth
strata
approx. depth (km)
Seattle
uplift
Tacoma
basin
c
Holocene B$_w$ horizon
Sand and gravel layers
Holocene B/E horizon
F1
F2
F3
Till
Fault
Inferred fault
Bottom of excavation
Pebbly layer,
gently folded

Figure 3.

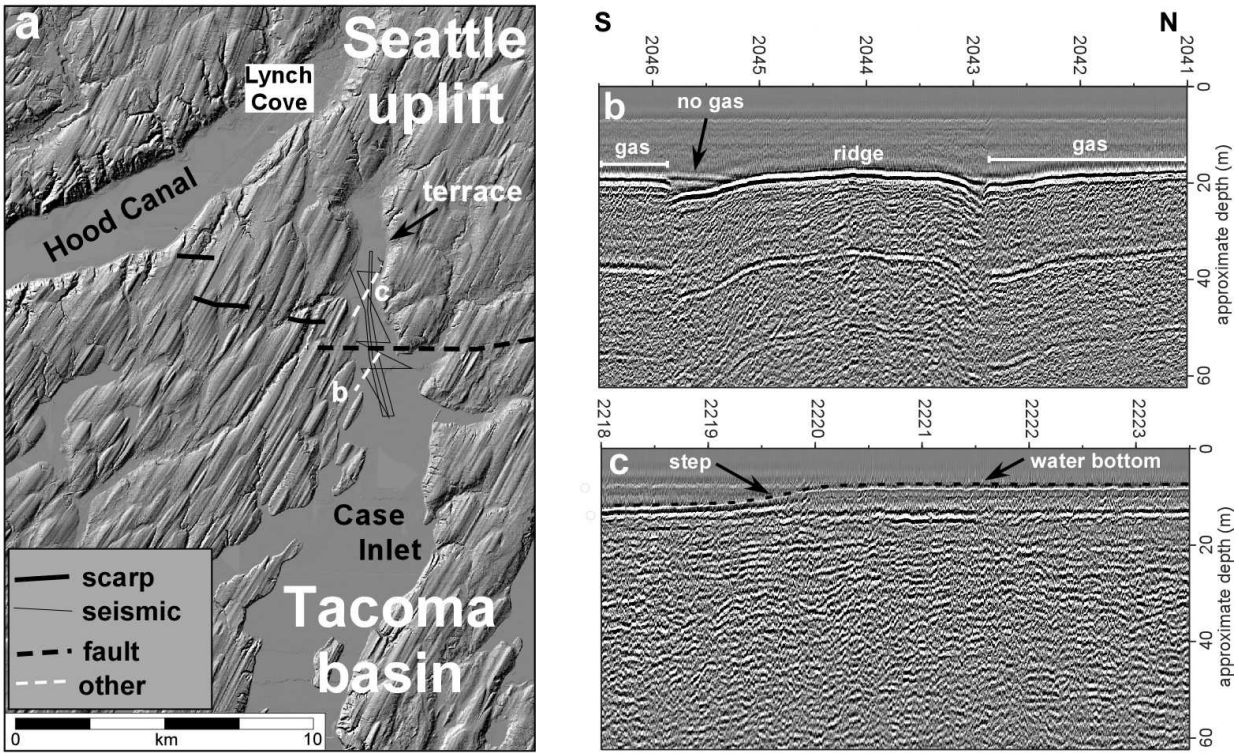
a
Seattle uplift
Lynch Cove
Hood Canal
terrace
c
b
Case Inlet
Tacoma basin
scarp
seismic
fault
other
0
km
10
S
N
2046
2045
2044
2043
2042
2041
b
no gas
gas
ridge
gas
approximate depth (m)
2218
2219
2220
2221
2222
2223
C
step
water bottom
approximate depth (m)

Figure 4.

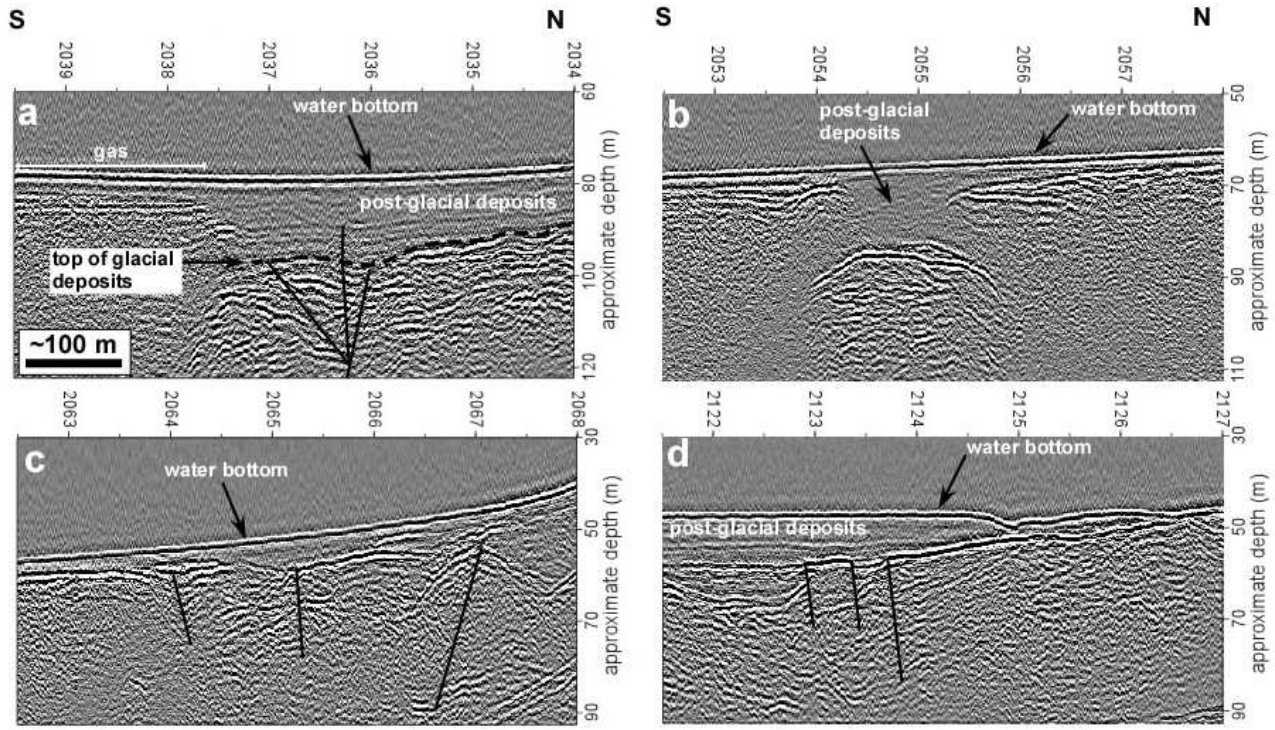
S
N
a
water bottom
gas
post-glacial deposits
top of glacial deposits
~100 m
approximate depth (m)
b
post-glacial deposits
water bottom
c
water bottom
d
water bottom
post-glacial deposits

Figure 5.

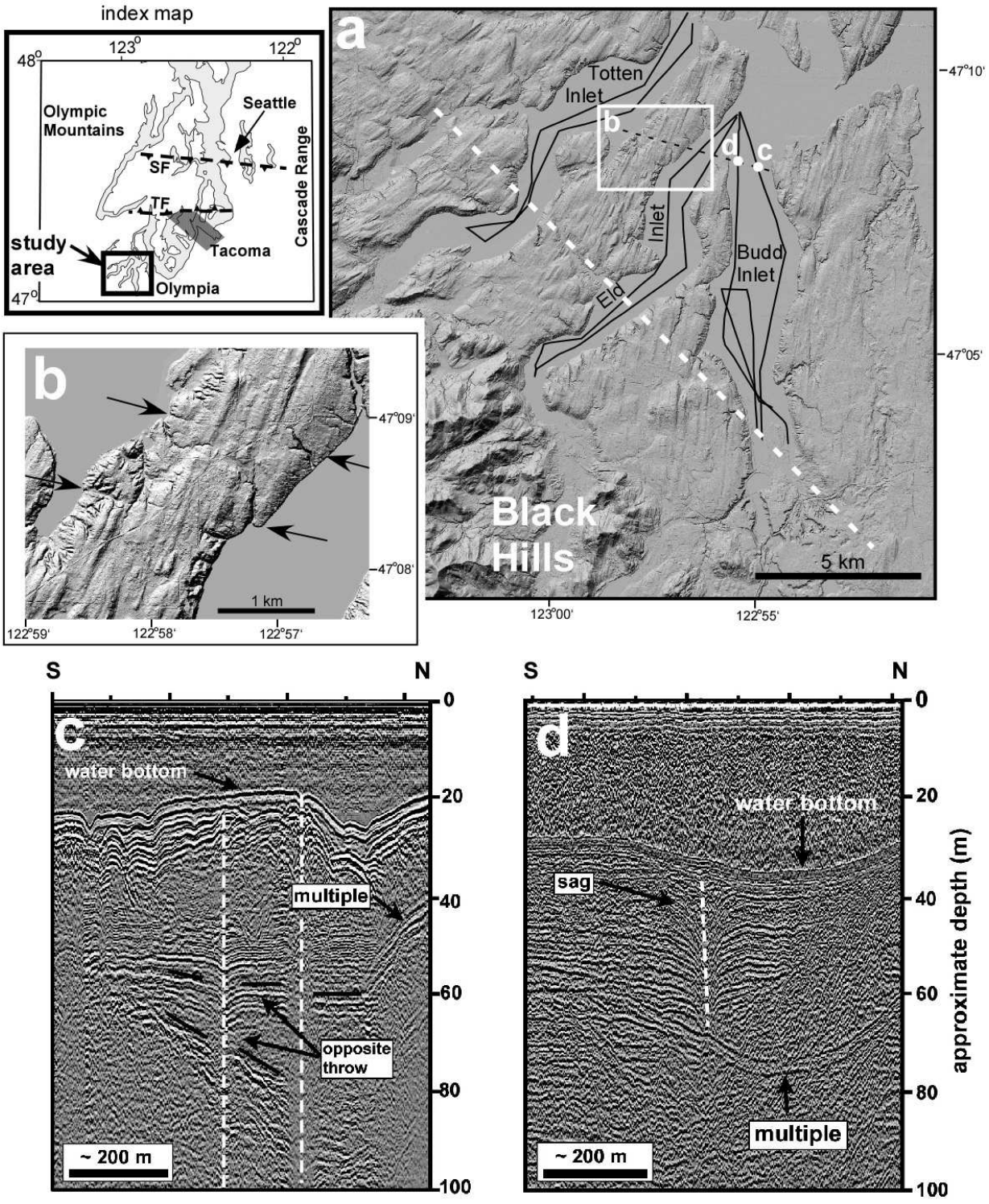
index map
48°
123°
122°
Olympic Mountains
Seattle
SF
TF
Cascade Range
study area
Tacoma
Olympia
47°
a
Totten Inlet
b
d
c
Eld Inlet
Budd Inlet
47°10'
47°05'
Black Hills
5 km
123°00'
122°55'
b
47°09'
47°08'
1 km
122°59'
122°58'
122°57'
S
N
c
water bottom
multiple
opposite throw
~ 200 m
0
20
40
60
80
100
d
water bottom
sag
multiple
~ 200 m
approximate depth (m)

Figure 6.